

A mass-optimized gravity tractor for asteroid deflection

Yohannes Ketema*

University of Minnesota, Minneapolis, MN 55455

A method for asteroid deflection that makes use of a spacecraft moving back and forth on a segment of a Keplerian orbit about the asteroid is studied with the aim of optimizing the initial gross mass of the spacecraft. The corresponding optimization problem is formulated as a discrete nonlinear optimal control problem where the parameters of the orbit segment are the control variables. A hypothetical asteroid deflection problem is solved numerically using the method of dynamic programming, and it is shown that a gravity tractor can be obtained that is significantly more efficient in terms of deflection attained per unit mass of the spacecraft, compared to similar gravity tractors in the literature.

*Associate Professor, Dept. of Aerospace Engineering and Mechanics, 107 Akerman Hall, 110 Union Street SE, Associate Fellow AIAA

Nomenclature

m_a	=	mass of asteroid
m_c	=	mass of spacecraft
μ_a	=	gravitational parameter for asteroid
μ_c	=	gravitational parameter for spacecraft
r_a	=	radius of asteroid
r	=	distance to spacecraft from asteroid center
α	=	ratio of spacecraft distance to asteroid radius
G	=	universal gravitational constant
θ	=	true anomaly on spacecraft orbit about asteroid
θ_b	=	bounding angle on spacecraft orbit about asteroid
Δv	=	impulsive velocity change
I	=	impulse imparted to asteroid
h	=	specific angular momentum for spacecraft orbit about asteroid
r_p	=	periapsis distance for spacecraft orbit about asteroid
r_{pm}	=	smallest allowable periapsis distance for spacecraft orbit about asteroid
e	=	eccentricity of spacecraft orbit about asteroid
γ	=	flight path angle for spacecraft orbit about asteroid
φ	=	plume half angle
Δt	=	time of flight on spacecraft orbit segment

- t_e = projected time of Earth-asteroid encounter
- v_a = orbital speed of asteroid
- a_a = semi-major axis of asteroid's orbit
- ζ = asteroid deflection measured at time of encounter
- r_0 = distance to apsis of gravity tractor orbit segment from asteroid center
- α = inverse of semi-major axis of gravity tractor orbit segment
- χ = universal variable for the time of flight on the gravity tractor orbit segment

I. Introduction

The prospect of Earth being impacted by an asteroid with potentially dire consequences to life on the planet calls for measures towards preventing or mitigating such a disaster. Thus several studies in the literature have been concerned with methods of asteroid deflection, i.e. altering the trajectories of asteroids by a required amount in order to avert a projected collision with Earth.

Three main approaches have been proposed with regards to asteroid deflection. These are kinetic impactors [1–6], nuclear interceptors [1, 7, 8], and gravity tractors [9–16]. Each method has characteristics that may make it suitable for the deflection of certain types and sizes of asteroids and possibly not for others. For example, kinetic impactors may be used with the aim of imparting an impulse to an asteroid to perturb its orbit without breaking it up into smaller pieces, thereby avoiding the creation of several objects that may impact Earth. In such a case, it is important that the asteroid be of a rocky type that will not easily disintegrate.

On the other hand, gravity tractors do not involve any direct contact with the asteroid. For this reason, they may be a viable approach for asteroid deflection when the asteroid is likely to break up upon impact. The force that gravity tractors can exert on an asteroid diminishes by the inverse square law. Thus, gravity tractors would generally be most effective on smaller asteroids [11].

Various forms of gravity tractors have been studied in the literature including the stationary gravity tractor [9] with canted thrusters in order to avoid impingement of the thruster plume on the asteroid; the displaced orbit (halo orbit) gravity tractor that gives a better thrust/fuel-mass ratio [17, 18]; and gravity tractors using solar sails [11, 19]. In

addition, the use of multiple gravity tractors in order to enhance the overall force on the asteroid has been studied in [14]. The navigation problem for such formations is studied in [20].

The gravity tractor that is considered in this paper is based on the method introduced in [15] and, as will be described further in the body of this paper, consists of a spacecraft that flies back and forth in a type of “restricted Keplerian motion” on an orbit segment about the asteroid. This gravity tractor can exert a significantly larger average force on the asteroid for a given spacecraft mass, while consuming less fuel, than for example a stationary gravity tractor with canted thrusters [9], or a displaced orbit gravity tractor [17].

The goal of this paper is to further improve upon the efficiency of the gravity tractor in ([15]). This is done by optimizing the gross initial mass of the spacecraft for a given amount of deflection by the projected date of encounter. The optimization takes into account variables that define the characteristics of the restricted Keplerian orbit segment as well as constraints that the orbit segment must satisfy so that a) the spacecraft does not impact the asteroid, b) there is no thruster plume impingement on the asteroid, and c) the time of flight on the orbit segment is sufficiently large for a realistic mission such that the spacecraft can properly orient and fire its thrusters at the rate of succession specified. In a numerical example consisting of a hypothetical asteroid deflection problem, it is shown that the optimization results in a decrease in the initial gross mass of the spacecraft that is in the order of 20% compared to a similar problem in [15] where no optimization was done.

Lastly, while the main focus of the work in this paper pertains to asteroid deflection in the case of a projected collision with Earth, the methods described would be applicable to related problems of asteroid redirection missions (ARM). In addition, the method described is in essence a way of “hovering” over an asteroid by remaining within given bounds on a Keplerian orbit while minimizing the required amount of fuel, and may therefore have broader applications, see e.g. [21].

The rest of this paper is organized as follows. In Section 2, a short description of the type of gravity tractor considered, i.e. a gravity tractor in restricted Keplerian motion about the asteroid, is given. In Section 3, the expressions for the deflection are expressed in terms of universal variables for the time of flight as these simplify the optimization analysis that requires a calculation of the time of flight on the restricted Keplerian orbit segment. Next in Section 4 a new set of variables are introduced to simplify the numerical analysis of the problem. The mass optimization problem is then formulated in Section 5, where the method of solution using dynamic programming (see e.g. [22, 23]) is also outlined. Lastly, in Section 6, a concrete example of the method is given using a hypothetical deflection problem of asteroid 2007 VK184.

II. Background

In this section a short introduction is given to the "dynamic" (i.e. not stationary with respect to the asteroid) gravity tractor that is the subject of the mass optimization study presented in the following sections. Details on the gravity tractor, which has been shown to be generally more efficient than a stationary gravity tractor, can be found in [15].

The dynamic gravity tractor consists of a spacecraft that moves back and forth along a segment of a Keplerian orbit about the asteroid as shown schematically in Figure 1. Assuming the orbit segment to be symmetric about the x axis, the average gravitational force on the asteroid from the spacecraft over one traversal of the orbit segment will be in the direction of the x axis. This is the force that is used to effect a perturbation of the asteroid's orbit about the Sun in order to avert a potential collision with Earth. The intersection between the orbit segment and the x axis, C , is an apsis of the orbit segment: periapsis in the case of a parabolic or hyperbolic orbit, and periapsis or apoapsis in the case of an elliptic orbit.

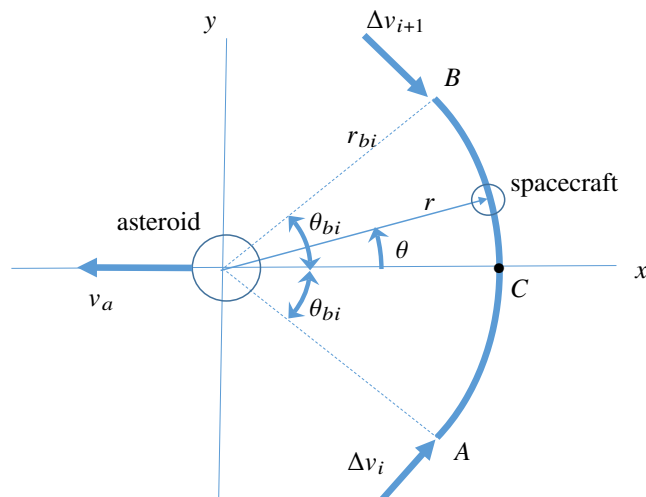


Fig. 1 The asteroid-spacecraft system.

In order to change its direction of motion on the orbit segment, i.e. at points A and B in Figure 1, the spacecraft fires its thruster, thereby effecting an impulsive velocity change denoted by Δv_{1i} and Δv_{2i} at points A and B , respectively. (The index i corresponds to the number of times the spacecraft has traversed the orbit segment, and reflects the fact that the properties of the orbit segment may be different for each time.) Thus, due to the fuel expenditure necessary for the impulsive velocity changes, the mass of the spacecraft decreases on successive orbit segments.

The successive times at which the spacecraft is at the ends of the orbit segment may be denoted by $t_i : i = 1, 2, 3, \dots$, such that the start time for the asteroid deflection mission is $t_s = t_1$ and the projected time of Earth-asteroid encounter is $t_e = t_N$. The mass of the spacecraft between the times t_i and t_{i+1} will be denoted by $(m_c)_i$.

The asteroid is generally on an elliptic orbit about the Sun. Therefore, its velocity is a function of time. However, during the short period of time between t_i and t_{i+1} the velocity may be assumed constant. This velocity will be denoted by v_{ai} .

With the above definitions, for the i 'th orbit segment, i.e. the one in the time interval $[t_i, t_{i+1}]$ with an angular momentum h_i and bounding angle θ_{bi} , the contribution to the deflection of the asteroid at the time of encounter t_e may be written as (see [15])

$$\Delta\zeta_i = -2G\kappa(m_c)_i v_{ai}(t_e - \bar{t}_i) \frac{\sin \theta_{bi}}{h_i} \quad (1)$$

where G is the universal gravitational constant and κ is a constant defined through

$$\kappa = \frac{3a_a}{\mu_S} v_a(t_e) \sin \psi, \quad (2)$$

with a_a being the semimajor axis of the asteroid's heliocentric orbit, μ_S is the gravitational parameter of the Sun, and ψ the angle between the heliocentric velocity of the asteroid and its relative velocity with respect to Earth at the projected time of encounter (see Figure 2). Further, \bar{t}_i is defined as

$$\bar{t}_i = \frac{t_i + t_{i+1}}{2}, \quad (3)$$

and can also be written as

$$\bar{t}_i = t_i + \frac{\Delta t_i}{2}, \quad (4)$$

where Δt_i is the time of flight on the i 'th orbit segment that can be calculated using Kepler's equation for the time of flight (see [24–26]) and will be discussed further below.

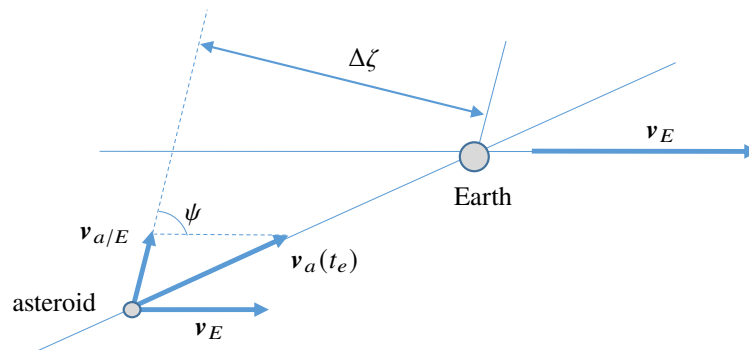


Fig. 2 Earth and the asteroid at the time of closest approach.

The mass of the spacecraft $(m_c)_i$ will change every time there is an impulsive velocity change Δv_i in accordance with the relation (see [27])

$$(m_c)_{(i+1)} = (m_c)_i e^{-\beta \Delta v_i} \quad (5)$$

where the parameter β is defined through

$$\beta = \frac{1}{I_{sp} g_0} \quad (6)$$

where I_{sp} is the specific impulse of the spacecraft's thruster and g_0 is the acceleration due to gravity at the surface of Earth [28]. The impulsive velocity change Δv_i corresponds to a change in the direction of the velocity at the ends of the orbit segment. Therefore

$$\Delta v_i = 2v_{bi} \quad (7)$$

where v_{bi} is the velocity of the spacecraft at the end of the orbit segment. Further, in the case of a small body such as an asteroid, as will be seen in Section 6 (see also [15]), v_{bi} is generally small. This implies that one can make the assumption

$$\beta \Delta v_i \ll 1 \quad (8)$$

and consequently (5) may be written in the form

$$(m_c)_{(i+1)} = (m_c)_i (1 - \beta \Delta v_i) \quad (9)$$

The total deflection caused at the time of encounter t_e due to the action of the gravity tractor from the initial time to a time t_k can be found as a sum of $\Delta \zeta_i$ which is given in (1). Denoting this cumulative deflection by ζ_k it follows that

$$\zeta_k = \sum_{i=1}^{k-1} \Delta \zeta_i \quad k > 1 \quad (10)$$

where $\zeta_1 = 0$, or using (1)

$$\zeta_k = \sum_{i=1}^{k-1} -2G\kappa(m_c)_i v_{ak}(t_e - \bar{t}_k) \frac{\sin \theta_{bk}}{h_k} \quad k > 1 \quad (11)$$

It is also useful to note that

$$\zeta_{k+1} = \zeta_k - 2G\kappa(m_c)_k v_{ak}(t_e - \bar{t}_k) \frac{\sin \theta_{bk}}{h_k} \quad (12)$$

thus giving a recursion formula for the deflection ζ_k .

A. Avoiding plume impingement

For the gravitational force from the spacecraft on the asteroid to be considered an external force that can have a net effect on the asteroid's heliocentric motion (and on the asteroid-spacecraft system's motion) it is necessary for the exhausts from the asteroid's thruster to leave the asteroid's sphere of influence without impinging on the asteroid, [9, 15].

Figure 3 illustrates for the i 'th orbit segment how the plume half-angle φ , the flight path angle γ_i , and the distance r_{bi} determine whether or not there is plume impingement. It follows from Figure(3) that the constraint that must be satisfied to avoid plume-impingement is

$$r_{bi} \sin\left(\frac{\pi}{2} - (\varphi - \gamma_i)\right) > r_a \quad (13)$$

or

$$r_{bi} \cos(\varphi - \gamma_i) > r_a \quad (14)$$

The flight path angle γ satisfies (see [27])

$$\tan \gamma = \frac{\dot{r}}{r\dot{\theta}} \quad (15)$$

Equivalently, noting that angular momentum h may generally be written in the form (see [27])

$$h = r^2\dot{\theta} \quad (16)$$

(15) may be written as

$$\tan \gamma = \frac{r\dot{r}}{h} \quad (17)$$

and therefore for the i 'th orbit segment

$$\tan \gamma_i = \frac{r_{bi}\dot{r}_{bi}}{h_i} \quad (18)$$

III. Universal variables

In optimizing the initial gross mass of the spacecraft for a given required deflection of the asteroid within a given time interval, it will be necessary to consider the time of flight on each orbit segment, i.e. from one end of the orbit segment to the other. (This will be described further in the next section.) Because one needs to consider elliptic, hyperbolic, or parabolic orbit segments in the general case, the time of flight calculation is simplified if one uses universal variables [24, 25]. This allows for the determination of the time of flight using the same expression for all three types of orbit segments. In this section, the required expressions for the time of flight are considered. In the development of these

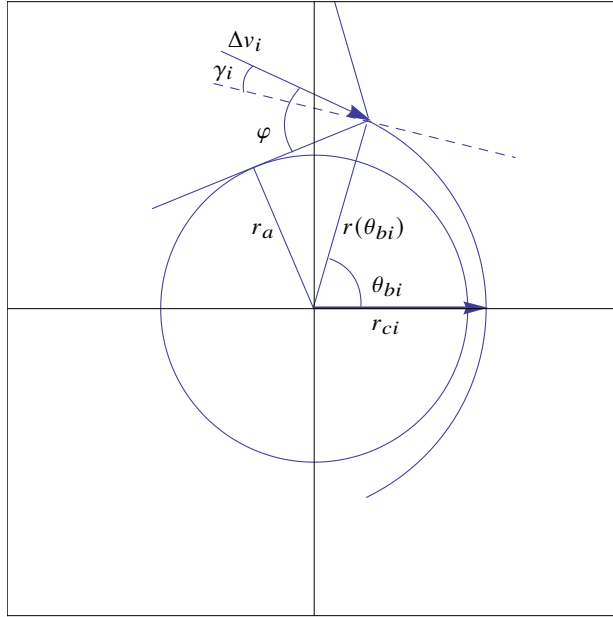


Fig. 3 Effect of plume angle on minimum periapsis radius.

expressions, the index i for the parameters pertaining to the i 'th orbit segment will be suppressed for brevity, and will be reinstated at the end of the section.

A. The time of flight

In terms of universal variables, the time of flight t from a point \mathbf{r}_0 on an orbit of semimajor axis a to a point \mathbf{r} on the same orbit may be written as [24, 25]

$$\sqrt{\mu}t = \chi^3 S(z) + \frac{\mathbf{r}_0 \cdot \mathbf{v}_0}{\sqrt{\mu}} \chi^2 C(z) + r_0 \chi (1 - zS(z)) \quad (19)$$

where χ is the universal variable for the time of flight, z is an auxiliary variable defined by

$$z = \frac{\chi^2}{a} \quad (20)$$

and where r_0 is defined through

$$r_0 = |\mathbf{r}_0|. \quad (21)$$

The Stumpff functions $C(z)$ and $S(z)$ are defined by

$$C(z) = \frac{1 - \cos \sqrt{z}}{z} \quad (22)$$

$$S(z) = \frac{\sqrt{z} - \sin \sqrt{z}}{(\sqrt{z})^3} \quad (23)$$

The value of r corresponding to a given value of χ may be written as (see e.g. [25])

$$r = \chi^2 C(z) + \frac{\mathbf{r}_0 \cdot \mathbf{v}_0}{\sqrt{\mu}} (1 - zS(z))\chi + r_0(1 - zC(z)) \quad (24)$$

To apply the above expressions to calculate the time of flight Δt between the two ends of the orbit segment, it may be noted that the time of flight is twice the time of flight from the apsis C to either end of the orbit segment (see Figure 1). Thus, in this case where the apsis of the orbit segment corresponds to r_0 , it follows that

$$\mathbf{r}_0 \cdot \mathbf{v}_0 = 0 \quad (25)$$

in (19) and (24). The time of flight between the two ends of the orbit segment may therefore be written as

$$\Delta t = \frac{2}{\sqrt{\mu}} [\chi^3 S(z) + r_0 \chi (1 - zS(z))] \quad (26)$$

Next, using (25) in (24), the distance from the center of mass of the asteroid to the end of the orbit segment may be written as

$$r = \chi^2 C(z) + r_0(1 - zC(z)) \quad (27)$$

Also, for later use, using (20), (22), and (25) in (27) yields the expression

$$r = a + (r_0 - a) \cos \sqrt{z} \quad (28)$$

B. The deflection in terms of universal variables

In the expressions for the time of flight using universal variables, the parameters r_0 , a , and χ (or z) characterize the orbit segment. Thus, for consistency in the overall problem, the deflection and conditions for avoiding plume-impingement derived in Section 2 can also be expressed in terms of universal variables.

In particular, regarding the deflection, the goal is to obtain an expression for the term $\sin \theta_{bk}/h_k$ in (11) and (12).

To this end, continuing to suppress the index i for the i 'th orbit segment, note that the radial component of the velocity may be written as (see [27])

$$\dot{r} = \pm \frac{\mu}{h} e \sin \theta \quad (29)$$

where '+' is used if C is periapsis and '-' is used if C is apoapsis of an elliptic orbit. The expression $\sin \theta_b/h$ in (1) may therefore be written as

$$\frac{\sin \theta}{h} = \pm \frac{\dot{r}}{\mu e} \quad (30)$$

Next, in terms of universal variables, \dot{r} may be written as (see [25])

$$\dot{r} = e \frac{\sqrt{a\mu}}{r} \cos \frac{\chi + c_0}{\sqrt{a}} \quad (31)$$

or

$$\dot{r} = e \frac{\sqrt{a\mu}}{r} \left[\cos \frac{\chi}{\sqrt{a}} \cos \frac{c_0}{\sqrt{a}} - \sin \frac{\chi}{\sqrt{a}} \sin \frac{c_0}{\sqrt{a}} \right] \quad (32)$$

where the constant c_0 satisfies the relations

$$e \sin \frac{c_0}{\sqrt{a}} = \frac{r_0}{a} - 1 \quad (33)$$

$$e \cos \frac{c_0}{\sqrt{a}} = \frac{\mathbf{r}_0 \cdot \mathbf{v}_0}{\sqrt{\mu a}} \quad (34)$$

Using (25) in (34) and substituting (33) and (34) into (32) now gives

$$\dot{r} = -\frac{\sqrt{a\mu}}{r} \left(\frac{r_0}{a} - 1 \right) \sin \frac{\chi}{\sqrt{a}} \quad (35)$$

Next, substituting (35) in (30) gives

$$\frac{\sin \theta}{h} = \mp \frac{1}{\mu e} \frac{\sqrt{\mu a}}{r} \left(\frac{r_0}{a} - 1 \right) \sin \sqrt{z} \quad (36)$$

Lastly, noting that

$$\frac{r_0}{a} - 1 = \mp e \quad (37)$$

where the top sign corresponds to the apsis C in Figure 1 being periapsis and the bottom sign to apoapsis (in the case of an elliptic orbit) (36) evaluated at the end of the orbit segment (i.e. $\theta = \theta_b$ etc.) may be written as

$$\frac{\sin \theta_b}{h} = \sqrt{\frac{a}{\mu}} \frac{\sin \sqrt{z_b}}{r_b} \quad (38)$$

which can be used in (1) to give (using parameter values for the i 'th orbit segment)

$$\Delta\zeta_i = -2G\kappa\nu_{ai}\sqrt{\frac{a_i}{\mu}}\frac{1}{r_{bi}}(m_c)_i(t_e - \bar{t}_i)\sin\sqrt{z_{bi}} \quad (39)$$

and using (10)

$$\zeta_k = \sum_{i=1}^{k-1} -2G\kappa\nu_{ai}\sqrt{\frac{a_i}{\mu}}\frac{1}{r_{bi}}(m_c)_i(t_e - \bar{t}_i)\sin\sqrt{z_{bi}} \quad (40)$$

C. The plume non-impingement constraint

Next, the condition to avoid plume impingement (14) will be expressed in terms of the orbit segment parameters r_{0i} , a_i , and χ_i (or z_i). Continuing to suppress the index i for simplicity and expanding the left hand side of (14) one obtains

$$r_b [\cos\varphi \cos\gamma_b + \sin\varphi \sin\gamma_b] > r_a \quad (41)$$

or

$$r_b \cos\gamma_b [\cos\varphi + \sin\varphi \tan\gamma_b] > r_a \quad (42)$$

Noting that the angular momentum can be found as (see [27])

$$h = rv \cos\gamma \quad (43)$$

the expression for $r_b \cos\gamma$ at the end of the orbit segment is obtained as

$$r_b \cos\gamma_b = \frac{h}{v_b} \quad (44)$$

which can be used in (42) along with (17) to yield

$$\frac{h}{v_b} \left[\cos\varphi + \sin\varphi \frac{r_b \dot{r}_b}{h} \right] > r_a \quad (45)$$

The angular momentum for the orbit segment may also be calculated at the apsis as

$$h = r_0 v_0 \quad (46)$$

and using this expression in (45) now gives

$$(r_0 v_0 \cos \varphi + r_b r_b \sin \varphi) > r_a v_b \quad (47)$$

Using the energy equation (written at the apsis) (see e.g. [27])

$$\frac{v_0^2}{2} - \frac{\mu}{r_0} = -\frac{\mu}{2a} \quad (48)$$

it follows that

$$v_0 = \sqrt{\frac{2\mu}{r_0} - \frac{\mu}{a}} \quad (49)$$

and similarly at the end points of the segment

$$v_b = \sqrt{\frac{2\mu}{r_b} - \frac{\mu}{a}} \quad (50)$$

The above expressions for v_0 and v_b can now be used in (47), and making use of (35), the plume non-impingement condition may be written as

$$r_0 \sqrt{\frac{2\mu}{r_0} - \frac{\mu}{a}} \cos \phi - \sin \phi \sqrt{\frac{\mu}{a}} (r_0 - a) \sin \frac{\chi_b}{\sqrt{a}} > r_a \sqrt{\frac{2\mu}{r_b} - \frac{\mu}{a}} \quad (51)$$

where, using (28), r_b is given by

$$r_b = a + (r_0 - a) \cos \sqrt{z_b} \quad (52)$$

To avoid problems with the numerical representation a in the case of a parabolic orbit segment (i.e. $a \rightarrow \infty$), a new variable α may be defined through (see e.g. [24],[25])

$$\alpha = \frac{1}{a} \quad (53)$$

Lastly, using (51)-(53) and defining the function

$$\Pi(r_0, \alpha, \chi_b) = r_a \sqrt{\frac{2\mu}{r_b(r_0, \alpha, \chi)} - \mu\alpha} - r_0 \sqrt{\frac{2\mu}{r_0} - \mu\alpha} \cos \phi + \sin \phi \sqrt{\mu\alpha} (r_0 - \frac{1}{\alpha}) \sin \chi_b \alpha^{\frac{1}{2}} \quad (54)$$

where

$$r_b(r_0, \alpha, \chi) = \alpha^{-1} + (r_0 - \alpha^{-1}) \cos \chi \sqrt{\alpha} \quad (55)$$

(51) may be written in the form

$$\Pi(r_0, \alpha, \chi_{bi}) < 0 \quad (56)$$

IV. A change of variables

As indicated earlier, the goal of the optimization analysis in the next section will be to choose the values of the orbital parameters r_{0k} , α_k , χ_{bk} , $k = 1 \dots N - 1$ such that a desired amount of deflection of the asteroid is achieved within a given amount of time and for the smallest possible initial mass of the spacecraft. This problem, that will be defined more precisely in the next section, takes on the form of a discrete-time nonlinear optimal control problem where the orbital parameters r_{0k} , α_k , and χ_{bk} constitute the $3(N - 1)$ control variables to be determined. Now, given that the duration of the mission is in the order of years, while the time of flight on the orbit segment is in the order of an hour, N will be large. For example, a 10-year-mission with the time of flight on an orbit segment $\Delta t = 30$ minutes gives $N = 175,200$. This is significant because it would generally make a numerical approach to solving the problem computationally intensive and slow.

The goal of this section is therefore to show that a different indexing of the variables can be used that leads to a problem that is numerically more tractable.

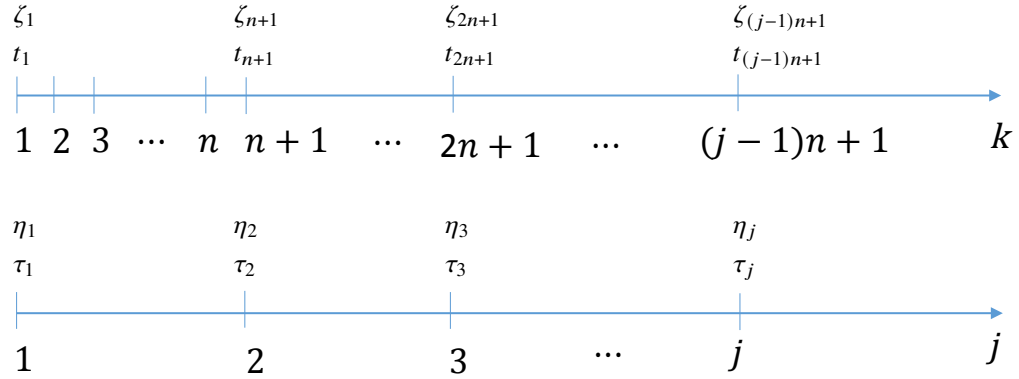


Fig. 4 Relation between the indices i and j .

Thus note that even though k was initially a natural choice as the index because it corresponds to the number of times the spacecraft has traversed the orbit segment, the variables ζ_k , \bar{t}_k , and m_k vary slowly with k , i.e. over a time scale in the order of years. In other words, it takes many traversions of the spacecraft's orbit segment before any significant

effect is observed in the variables ζ_k , \bar{t}_k , and m_k . At the same time, the optimal values of the control variables at a given time will generally depend on the values of ζ_k , t_k , and m_k . This means that the control variables will also vary slowly with k and do not need to be updated after every traversal of the orbit segment. Instead, they may be assumed to remain constant for some chosen increment of k , say n . Hence, a new “slowly varying” index j can be defined such that j increases by one for an increase of k by n (see Figure 4) or

$$j = \text{int}\left(\frac{k-1}{n}\right) + 1 \quad (57)$$

where $\text{int}(\cdot)$ is the integer part of the argument, and both j and k start at 1. For ease of reference, new state variables η_j , τ_j , and m_j corresponding to index j may be defined. These variables are related to the original state variables through

$$\eta_j = \zeta_{(j-1)n+1} \quad (58)$$

$$\tau_j = t_{(j-1)n+1} \quad (59)$$

$$m_j = (m_c)_{(j-1)n+1} \quad (60)$$

Figure 4 illustrates the definition of η_j and τ_j ; the definition for m_j is analogous. Similarly, the control variables corresponding to the index j are defined as \tilde{r}_{0j} , $\tilde{\alpha}_j$, and $\tilde{\chi}_{bj}$ as follows:

$$\tilde{r}_{0j} = r_{(j-1)n+1} \quad (61)$$

$$\tilde{\alpha}_j = \alpha_{(j-1)n+1} \quad (62)$$

$$\tilde{\chi}_{bj} = \chi_{b[(j-1)n+1]} \quad (63)$$

Conversely, for $k \in [(j-1)n+1, jn]$

$$r_{0k} = \tilde{r}_{0j} \quad (64)$$

$$\alpha_k = \tilde{\alpha}_j \quad (65)$$

$$\chi_{bk} = \tilde{\chi}_{bj} \quad (66)$$

A. Recursion formulas

As with the original state variables, state propagation equations for the variables η_j , τ_j , and m_j will need to be obtained. This can be done by evaluating the corresponding changes in the variables ζ_k , t_k , and $(m_c)_k$ as will be shown

in this section.

1. The time variable:

The recursion equation for the time variable takes

$$\tau_{j+1} = \tau_j + n\Delta\tilde{t}_j \quad (67)$$

where $\Delta\tilde{t}_j$ denotes the time of flight on each orbit segment between the times of j and $j + 1$, or equivalently between $k = (n - 1)j + 1$ and $k = nj$. This time of flight is given by (26) which can be written in terms of the variables \tilde{r}_{0j} , $\tilde{\alpha}_j$, and $\tilde{\chi}_j$ by using (20) and (53) to yield

$$\Delta\tilde{t}_j = \frac{2}{\sqrt{\mu}} \left[\tilde{\chi}_{bj}^3 \mathcal{S}(\tilde{\chi}_{bj}^2 \tilde{\alpha}_j) + \tilde{r}_{0j} \tilde{\chi}_{bj} (1 - \tilde{\chi}_{bj}^2 \tilde{\alpha}_j \mathcal{S}(\tilde{\chi}_{bj}^2 \tilde{\alpha}_j)) \right] \quad (68)$$

2. The spacecraft mass:

To determine the change in the mass of the spacecraft between time j and $j + 1$ we note that the thrusters will have been fired n times, i.e. (9) is used n times with a constant value of Δv_i that corresponds to the parameters of the orbit segment. Denoting this constant value by $\Delta\tilde{v}_j$ for this interval gives

$$m_{j+1} = m_j (1 - \beta \Delta\tilde{v}_j)^n \quad (69)$$

or, in keeping with the linearization used in obtaining (9)

$$m_{j+1} = m_j (1 - n\beta \Delta\tilde{v}_j) \quad (70)$$

3. The deflection

Using (58) and (40) it follows that

$$\eta_j = \sum_{i=1}^{(j-1)n} -2Gv_{ai} \sqrt{\frac{a_i}{\mu}} \frac{1}{r_{bi}} (m_c)_i (t_e - \bar{t}_i) \sin \sqrt{z_{bi}} \quad (71)$$

which implies that

$$\eta_{j+1} = - \sum_{i=1}^{nj} 2Gv_{ai} \sqrt{\frac{a_i}{\mu}} \frac{1}{r_{bi}} (m_c)_i (t_e - \bar{t}_i) \sin \sqrt{z_{bi}} \quad (72)$$

Using (72) together with (71) now gives

$$\eta_{j+1} = \eta_j - \sum_{i=n(j-1)+1}^{nj} -2Gv_{ai} \sqrt{\frac{a_i}{\mu}} \frac{1}{r_{bi}} (m_c)_i (t_e - \bar{t}_i) \sin \sqrt{z_{bi}} \quad (73)$$

and, noting that the orbital parameters of the orbit segment have constant values within the summation interval given by (64)-(66), it follows that

$$\eta_{j+1} = \eta_j - 2G\tilde{v}_{aj} \sqrt{\frac{\tilde{a}_j}{\mu}} \frac{1}{\tilde{r}_{bj}} \sin \sqrt{z_{bj}} \sigma_j \quad (74)$$

where

$$\sigma_j = \sum_{i=n(j-1)+1}^{nj} (m_c)_i (t_e - \bar{t}_i) \quad (75)$$

has been defined for brevity. In order to evaluate the sum in (75), explicit expressions for the dependence of $(m_c)_i$ and \bar{t}_i on i are needed. Hence, it is first noted that the times of the impulsive thrusts t_i within the summation interval $[n(j-1)+1, nj]$ may be written as

$$t_i = \tau_j + (i - n(j-1) - 1)\Delta\tilde{t}_j, \quad i \in [(j-1)n+1, nj] \quad (76)$$

and that the time of flight Δt_i for each orbit segment within the summation interval is

$$\Delta t_i = \Delta\tilde{t}_j \quad (77)$$

Further, using (4) it follows that

$$\bar{t}_i = \tau_j + (i - n(j-1) - 1)\Delta\tilde{t}_j + \frac{\Delta\tilde{t}_j}{2}; \quad i \in [(j-1)n+1, jn] \quad (78)$$

Similarly for the mass, using (9)

$$(m_c)_i = (m_c)_{n(j-1)+1} (1 - (i - n(j-1) - 1)\beta\Delta\tilde{v}_j); \quad i \in [(j-1)n+1, jn] \quad (79)$$

or using (60)

$$(m_c)_i = m_j (1 - (i - n(j-1) - 1)\beta\Delta\tilde{v}_j); \quad i \in [(j-1)n+1, jn] \quad (80)$$

Introducing a new index q through

$$q = i - n(j - 1) - 1 \quad (81)$$

and using (78) and (80) allows (75) to be written in the form

$$\sigma_j = \sum_{q=0}^{n-1} m_j (1 - q\beta\Delta\tilde{v}_j) (t_e - \tau_j - q\Delta\tilde{t}_j - \frac{\Delta\tilde{t}_j}{2}) \quad (82)$$

or, after rearranging terms,

$$\sigma_j = (t_e - \tau_j - \frac{\Delta\tilde{t}_j}{2}) m_j \sum_{q=0}^{n-1} (1 - q\beta\Delta\tilde{v}_j) - m_j \Delta\tilde{t}_j \sum_{q=0}^{n-1} q (1 - q\beta\Delta\tilde{v}_j) \quad (83)$$

Finally, evaluating the sums gives

$$\sigma_j = m_j (t_e - \tau_j - \frac{\Delta\tilde{t}_j}{2}) \left(n - \frac{n(n-1)}{2} \beta\Delta\tilde{v}_j \right) + m_j \Delta\tilde{t}_j \left(\frac{n(n-1)(2n-1)}{6} \beta\Delta\tilde{v}_j - \frac{n(n-1)}{2} \right) \quad (84)$$

As has been discussed earlier, t_e which is a time in the order of years is much larger than $\Delta\tilde{t}_j$ which is in the order of minutes. It is therefore possible to neglect the term $\frac{\Delta\tilde{t}_j}{2}$ in the expression $(t_e - \tau_j - \frac{\Delta\tilde{t}_j}{2})$ in (84). Next, substituting (84) into (74) and using (20) and (53) yields

$$\eta_{j+1} = \eta_j - 2G\tilde{v}_{aj} \sqrt{\frac{\tilde{\alpha}_j}{\mu}} \frac{1}{\tilde{r}_{bj}} \sin \sqrt{\tilde{z}_{bj}} \times \left[m_j (t_e - \tau_j) \left(n - \frac{(n-1)}{2} \beta\Delta\tilde{v}_j \right) + m_j \Delta\tilde{t}_j \left(\frac{n}{6} (n-1)(2n-1) \beta\Delta\tilde{v}_j - \frac{n(n-1)}{2} \right) \right] \quad (85)$$

B. The non-impingement constraint for the plume

Finally, the plume non-impingement constraint (56) needs to be specified for the j 'th set of orbit segments, i.e. for $i \in [(j-1)n+1, jn]$. However, this is simply a matter of replacing the control variables r_{0i} , α_i , and χ_i in (56) with the new control variables defined in this section \tilde{r}_{0j} , $\tilde{\alpha}_j$, and $\tilde{\chi}_j$ by using (64)-(66). The plume non-impingement constraint is therefore written as

$$\Pi(\tilde{r}_{0j}, \tilde{\alpha}_j, \tilde{\chi}_{bj}) < 0 \quad (86)$$

V. Mass optimization

The analysis in the rest of this paper is concerned with choosing the orbital parameters for the Keplerian orbit segment around the asteroid for each value of the discrete time τ_j , in order to effect a desired deflection at the projected time of Earth-encounter, while minimizing the required initial mass.

As will be further detailed below, the following approach will be well-suited in conjunction with the use of the method of dynamic programming: For a range of values of initial mass of the spacecraft, the largest deflection that can be obtained by the time of the projected encounter is calculated. From this optimal mapping of initial mass to largest deflection, the smallest mass that results in the required deflection is picked. Thus in the optimization process itself, the goal is to minimize the deflection (with a direction corresponding to a negative value). However, only deflections that can be attained before the projected time of encounter are of value. Thus the cost function will include a large penalty for final times greater than t_e . The cost function may therefore be defined as

$$J = \eta_N + Kf(t_N) \quad (87)$$

where K is chosen so that $K \gg \eta_N$ and

$$f(t_N) = \begin{cases} 0 & t_N \leq t_e \\ 1 & t_N > t_e \end{cases} \quad (88)$$

A. The control variables

The parameters that characterize the orbit segment at each index j are the distance r_{0j} from the center of the asteroid to the apsis C , the inverse of the semimajor axis $\tilde{\alpha}_j$, and the universal variable at the end of the orbit segment $\tilde{\chi}_{bj}$ (or equivalently \tilde{z}_{bj}). These are therefore the control variables that need to be determined at each index j . The $\tilde{\cdot}$'s in these notations were introduced in order to differentiate these quantities from the ones that were updated after every traversal of the orbit segment. From this point on, however, the $\tilde{\cdot}$'s can be dropped for simplicity; no confusion should arise as the original variables will no longer be in use.

For use in what follows, the control vector may be defined as

$$\mathbf{u}_j = [r_{0j}, \alpha_j, \chi_j]^T \quad (89)$$

B. The state variables

The recursion equations for the state variables m_j , τ_j , and η_j were expressed in (70), (67), and (85), respectively. Defining for brevity the functions

$$Z(\eta_j, \tau_j, m_j; r_{0j}, \alpha_j, \chi_{bj}) = -2G\tilde{v}_{aj} \sqrt{\frac{\tilde{a}_j}{\mu}} \frac{1}{r(r_{0j}, \alpha_j, \chi_{bj})} \sin \sqrt{\tilde{z}_{bj}} \quad (90)$$

and

$$S(\eta_j, \tau_j, m_j; \Delta v_j, \alpha_j, \chi_j) = \left[m_j \left(t_e - \tau_j - \frac{\Delta \tilde{t}_j}{2} \right) \left(n - \frac{(n-1)}{2} \beta \Delta v_j \right) + \right. \quad (91)$$

$$\left. m_j \Delta \tilde{t}_j \left(\frac{n}{6} (n-1) (2n-1) \beta \Delta v_j - \frac{n(n-1)}{2} \right) \right] \quad (92)$$

where Δv_j is calculated using (7) and (50), (85) may be written as

$$\eta_{j+1} = \eta_j + Z(\eta_j, \tau_j, m_j; \Delta v_j, \alpha_j, \chi_j) S(\eta_j, \tau_j, m_j; \Delta v_j, \alpha_j, \chi_j) \quad (93)$$

Next, using (67) and (70) the three state equations can be put in the form

$$\begin{bmatrix} \eta_{j+1} \\ \tau_{j+1} \\ m_{j+1} \end{bmatrix} = \begin{bmatrix} \eta_j + Z(\eta_j, \tau_j, m_j; \Delta v_j, \alpha_j, \chi_j) S(\eta_j, \tau_j, m_j; \Delta v_j, \alpha_j, \chi_j) \\ \tau_j + n \Delta \tilde{t}_j \\ m_j (1 - n \beta \Delta v_j) \end{bmatrix} \quad (94)$$

The j' th state vector \mathbf{x}_j may be defined through

$$\mathbf{x}_j = [\eta_j, \tau_j, m_j]^T \quad (95)$$

and the state propagation equations may be written as

$$\mathbf{x}_{j+1} = \mathbf{f}(\mathbf{x}_j, \mathbf{u}_j) \quad (96)$$

where, using (94), the vector function $\mathbf{f}(\mathbf{x}_j, \mathbf{u}_j)$ is defined through

$$\mathbf{f}(\mathbf{x}_j, \mathbf{u}_j) = \begin{bmatrix} \eta_j + Z(\eta_j, \tau_j, m_j; \Delta v_j, \alpha_j, \chi_j)S(\eta_j, \tau_j, m_j; \Delta v_j, \alpha_j, \chi_j) \\ \tau_j + n\Delta\tilde{t}_j \\ m_j(1 - n\beta\Delta v_j) \end{bmatrix} \quad (97)$$

C. Constraints on the controls

As discussed in Section 4, the controls \tilde{r}_{0j} , a_j , and χ_j are required to satisfy the following constraints:

1. No plume impingement

This requirement has already been discussed in Section 3.4 and stated in (86).

2. No impact

In addition to the avoidance of plume-impingement, it must be required that the orbit segment itself does not intersect the asteroid. Thus if the apsis point at the distance r_0 from the center of the asteroid is periapsis, then the no impact condition is

$$r_{0j} > r_a \quad (98)$$

or

$$r_a - r_{0j} < 0 \quad (99)$$

If on the other hand the orbit segment is elliptic and the apsis point is apoapsis, the points on the orbit segment closest to the asteroid are the end points at a distance of r_b from the center of the asteroid. In this case the no impact condition becomes

$$r_b > r_a \quad (100)$$

However, this condition is already satisfied due to the no plume-impingement condition given in (14) and therefore does not need to be imposed separately.

3. Sufficient time between impulsive velocity changes

The assumption of impulsive thrusts used in the analysis in this paper implies that the time of flight is much larger than the time required in practice to impart the required Δv . Hence, a lower-bound constraint on the time of flight is

needed and may be written as

$$\Delta \tilde{t}_j > t_{min} \quad (101)$$

or using (68) and defining the function

$$\begin{aligned} \Upsilon(r_{0j}, \alpha_j, \chi_{bj}) = \\ t_{min} - \frac{2}{\sqrt{\mu}} \left[\tilde{\chi}_j^3 S(\tilde{\chi}_j^2 \tilde{\alpha}_j) + \tilde{r}_{0j} \tilde{\chi}_{bj} (1 - \tilde{\chi}_{bj}^2 \tilde{\alpha}_j S(\tilde{\chi}_{bj}^2 \tilde{\alpha}_j)) \right] \end{aligned} \quad (102)$$

the constraint on the time of flight becomes

$$\Upsilon(\Delta v_j, \alpha_j, \chi_{bj}) < 0 \quad (103)$$

The three constraints on the controls that have been described may be expressed more compactly if one defines the vector

$$G(r_{0j}, \alpha_j, \chi_j) = \begin{bmatrix} r_a - r_{0j} \\ \Gamma(r_{0j}, \alpha_j, \chi_{bj}) \\ \Upsilon(r_{0j}, \alpha_j, \chi_{bj}) \end{bmatrix} \quad (104)$$

to give the overall constraint

$$G(r_{0j}, \alpha_j, \chi_{bj}) < \mathbf{0} \quad (105)$$

D. Dynamic programming

Using (87) it may be noted that the performance index is in the form*.

$$J = \phi(\mathbf{x}_\nu) \quad (106)$$

where ν is the final value of the index j . This problem is straightforward to solve using the numerical approach of dynamic programming [22, 23]. Thus, for each index j in (106) a discretized set of values of the state variable \mathbf{x}_j and the control variable \mathbf{u}_j are considered. The set of values of \mathbf{x}_j corresponding to a grid formed by discretizing the

*More generally the performance index would have the form $J = \phi(\mathbf{x}_\nu) + \sum_{j=0}^{\nu-1} \mathcal{L}(\mathbf{x}_j, \mathbf{u}_j)$, i.e. would also depend on the history of the state and control variables (see e.g. [22])

deflection, mass, and time variables that may be denoted as

$$\bar{\eta}_j = \{\eta_j^1, \eta_j^2, \eta_j^3, \dots, \eta_j^{q_\eta}\} \quad (107)$$

$$\bar{\tau}_j = \{\tau_j^1, \tau_j^2, \tau_j^3, \dots, \tau_j^{q_\tau}\} \quad (108)$$

$$\bar{m}_j = \{m_j^1, m_j^2, m_j^3, \dots, m_j^{q_m}\} \quad (109)$$

where q_η , q_τ , and q_m denote the lengths of the arrays used for the variables $\bar{\eta}$, $\bar{\tau}$, and \bar{m} , respectively.

Similarly, \mathbf{u}_j will have a set of values on a grid formed by discretized values of \bar{r}_0 , $\bar{\alpha}$, and $\bar{\chi}$ defined as

$$\bar{r}_{0j} = \{r_{0j}^1, r_{0j}^2, r_{0j}^3, \dots, r_{0j}^{q_{r_0}}\} \quad (110)$$

$$\bar{\alpha}_j = \{\alpha_j^1, \alpha_j^2, \alpha_j^3, \dots, \alpha_j^{q_\alpha}\} \quad (111)$$

$$\bar{\chi}_{bj} = \{\chi_{bj}^1, \chi_{bj}^2, \chi_{bj}^3, \dots, \chi_{bj}^{q_\chi}\} \quad (112)$$

where q_{r_0} , q_α , and q_χ denote the lengths of the arrays \bar{r}_0 , $\bar{\alpha}$, and $\bar{\chi}$, respectively.

The optimization procedure is started by calculating and storing the contribution from each of the final states \mathbf{x}_ν to the performance index on a trajectory that would end at that final state. This value may be denoted as

$$J_\nu(\mathbf{x}_\nu) = \phi(\mathbf{x}_\nu) \quad (113)$$

Next, the index $j = \nu - 1$ is considered for the discretized set of states $\mathbf{x}_{\nu-1}$. At each value of $\mathbf{x}_{\nu-1}$ all possible combinations of the controls are used to determine the values of \mathbf{x}_ν that they would result in, i.e., using (96)

$$\mathbf{x}_\nu = \mathbf{f}(\mathbf{x}_{\nu-1}, \mathbf{u}_{\nu-1}) \quad (114)$$

The total cost associated with such a trajectory is calculated as

$$J_{\nu-1,\nu}(\mathbf{x}_{\nu-1}, \mathbf{u}_{\nu-1}) = J_\nu(\mathbf{x}_\nu) \quad (115)$$

Of these values, the minimum is calculated for each $\mathbf{x}_{\nu-1}$ and is denoted as

$$J_{\nu-1,\nu}^*(\mathbf{x}_{\nu-1}) = \min_{\mathbf{u}_{\nu-1}} J_\nu(\mathbf{x}_\nu) \quad (116)$$

In the process, the corresponding optimal value of $\mathbf{u}_j(\mathbf{x}_{\nu-1})$ is calculated and stored.

The procedure is now repeated for the states $\mathbf{x}_{\nu-2}$ by determining the controls that minimize the cost on trajectories from each $\mathbf{x}_{\nu-2}$ to corresponding final states \mathbf{x}_ν , and, considering trajectories to the states $\mathbf{x}_{\nu-1}$. The minimal cost for each $\mathbf{x}_{\nu-2}$ to go from $j = \nu - 2$ to $j = \nu$ may be denoted as

$$J_{\nu-2,\nu}^*(\mathbf{x}_{\nu-2}) = \min_{\mathbf{u}_{\nu-2}} J_\nu(\mathbf{x}_{\nu-1}) \quad (117)$$

A repeat of the above procedure leads to a recursion formula in the form

$$J_{\nu-k,\nu}^*(\mathbf{x}_{\nu-k}) = \min_{\mathbf{u}_{\nu-k}} J_{\nu-(k-1),\nu}^*(\mathbf{f}(\mathbf{x}_{\nu-k}, \mathbf{u}_{\nu-k})) \quad (118)$$

The end result of the algorithm is that for $k = \nu - 1$ i.e. $\nu - k = 1$, the optimal cost $J_{1,\nu}^*(\mathbf{x}_1)$ is obtained for each value of \mathbf{x}_1 , i.e. the optimal cost on a trajectory that starts at state \mathbf{x}_1 and the associated controls \mathbf{u}_j^* . At this point, using the constraints that $\eta_1 = 0$ and $\tau_1 = 0$, only the various possible values of initial mass need be considered. This defines a map from the initial values of gross spacecraft mass to the corresponding deflection that minimizes J .

$$\eta_\nu = P(m_1) \quad (119)$$

The value of m_1 that corresponds to $\eta_\nu = d_r$ can now be calculated by interpolation.

E. Choosing the number of steps

As described above, ν is the final value of the index j . Due to the varying values of Δt_j , however, ν cannot be simply derived from the value of the final time t_e . Instead, ν can be chosen to be sufficiently large to allow τ_j to reach t_e for some value of $j = j_f$. Now, once $\tau_j \geq t_e$, there is no need to propagate the state variables any more and they can be assumed to stay constant at their values at $j = j_f$.

VI. Example: Deflection of Asteroid VK184

In order to exemplify the optimization procedure detailed above, and to evaluate the merits of the approach, a concrete example is presented in this section concerning the hypothetical deflection of an asteroid. The asteroid considered is 2007 VK184, which is also considered in [15] and [12] and will therefore allow for a comparison of the results in these works to those in the current paper.

Asteroid 2007 VK184 is projected to have a close encounter with Earth in June 2048, with virtually no risk of

collision. The mass and radius of the asteroid are $m_a = 3.3 \times 10^9$ kg and $r_a = 65$ m, respectively [29]. The semimajor axis of the asteroid's orbit is $a_a = 1.7262AU$ [30].

For the parameters ψ , $v_a(t_e)$, and a_a in (2) it is shown in [15] that

$$\psi = 0.829 \text{ rad} \quad (120)$$

$$v_a(t_e) = 35,500 \text{ m/s} \quad (121)$$

which allows for the calculation of κ as

$$\kappa = 1.528 \times 10^{-4} \text{ s/m} \quad (122)$$

For the sake of specificity, it will be assumed in this section that the encounter time $t_e = 10$ years (i.e. the deflection maneuvers would start in the year 2038) and that the smallest allowable time of flight on the orbit segment is $\Delta t_{min} = 1800$ s.

Denoting a one-dimensional array \bar{p} of N equally spaced values with first value p_1 and last value p_N by

$$\bar{p} = \mathcal{A}(p_1, p_N, N) \quad (123)$$

the grid of values for $\bar{\eta}$, $\bar{\tau}$, and \bar{m} in the dynamic programming algorithm are taken to be

$$\bar{\eta} = \mathcal{A}(0, -2.4 \times 10^6 \text{ m}, 20) \quad (124)$$

$$\bar{\tau} = \mathcal{A}(0, 10 \text{ yrs}, 20) \quad (125)$$

$$\bar{m} = \mathcal{A}(100, 3600 \text{ kg}, 20) \quad (126)$$

Similarly, a grid of values can be chosen for the controls. However, iterative numerical studies show that the optimal value of r_0 is its smallest allowable value, i.e. r_e , the radius of the asteroid. This may be explained by the fact that a small r_0 will generally increase the gravitational force. In the interest of computational time and higher resolution for the other control variables, r_0 is set to 65 m, the radius of the asteroid. For the other two control variables

$$\bar{\alpha} = \mathcal{A}(0.012/\text{m}, 0.015/\text{m}, 20) \quad (127)$$

$$\bar{\chi} = \mathcal{A}(6 \text{ m}^{1/2}, 10 \text{ m}^{1/2}, 30) \quad (128)$$

The array sizes for $\bar{\alpha}$ and $\bar{\chi}$ were chosen iteratively in order to give the resolution required to adequately describe the

variations of the variables as seen in Figure 6.

Lastly, the parameter n in (84) is set to $n = 700$. This choice is based on an assumption of $\Delta t_j \approx 1800$ s (the upper bound set) meaning that the total time corresponding to a unit increment of j is roughly 1.26×10^6 s or about 14 days. This time interval is about 1.6% of the period of the asteroid (2.34 years), making the assumption of a constant asteroid velocity during the time interval reasonable.

Applying dynamic programming as described above, the optimal trajectory starting from each admissible initial state of $\eta = 0$ m, $\tau = 0$ s, and $m \in \bar{m}$ is calculated. Each value of the initial mass will result in a corresponding final value of the deflection η_f . The trajectory of interest is one that would result in a final value of $\eta = dr$. The initial mass corresponding to that trajectory can now be found by interpolation.

The time dependence for the corresponding optimal solution of the state variables is shown in Figures (5). In particular it is seen from Figure (5)(c) that the optimal initial and final spacecraft masses are 1150 kg and 540 kg, respectively.

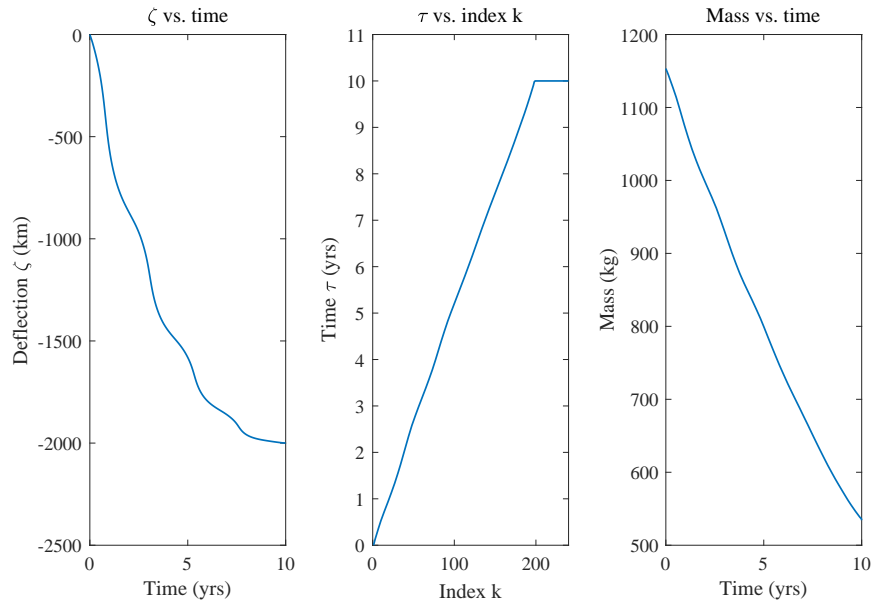


Fig. 5 Example time dependence of the state variables η , τ , and m for the case of $t_e = 10$ years.

Similarly, Figure 6 shows the optimal time dependence of the control variables r_0 , α , and χ . The piecewise constant nature of the dependence for α , and χ is a result of the discretization process for dynamic programming that has been described above.

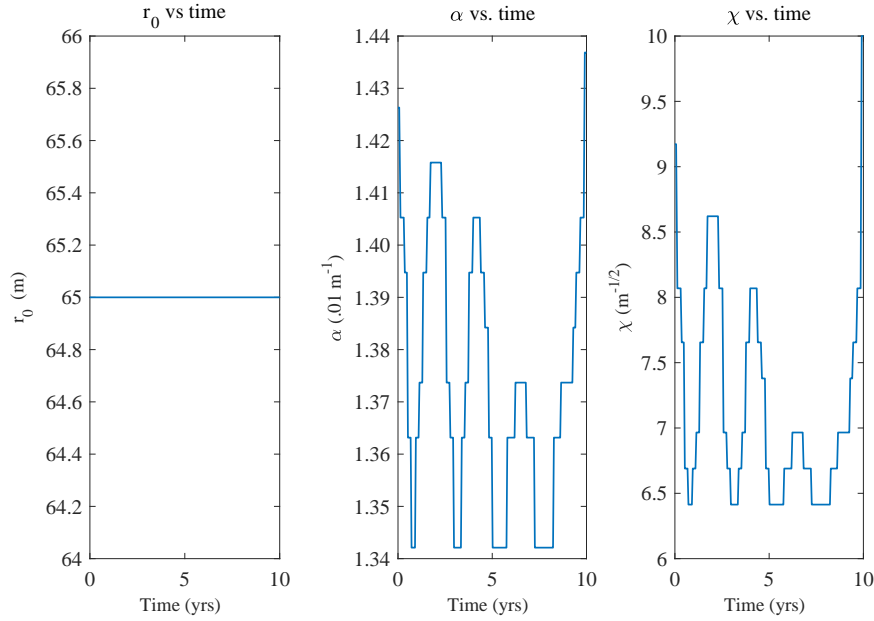


Fig. 6 Time dependence of the control variables r_0 , α , and χ for the case of $t_e = 10$ years.

The overall time dependence of the control variables α , and χ may be understood in terms of the varying velocity of the asteroid. In Figure 7 the time-dependence of the asteroid velocity is shown along with the time-dependence of χ (note that α has the same qualitative time-dependence as χ). It follows that χ (and therefore α) have their smallest and largest values at the maximum and minimum asteroid velocities, respectively. A small α corresponds to a larger (higher energy) orbit where the velocities, and therefore changes in velocities, at the ends of the orbit segment are large. Correspondingly, a small χ means that the Δv 's are being applied at a higher rate, increasing the average force. It may be concluded that the overall control effort is larger when the asteroid velocity is larger, and vice versa. This is a result of the way in which a contribution to the deflection $\Delta\zeta_k$ depends on the asteroid velocity as expressed in (39), making it more efficient to exert a larger force when the asteroid velocity is large.

To study the dependence of the required initial spacecraft mass on the lead time for the start of the mission, the optimal trajectories can be obtained for a range of values of t_e . Figure (8) shows this dependence of the optimal initial and final masses on the lead time.

Lastly Figure (9) shows the dependence of the amount of fuel that is required as a function of the lead time.

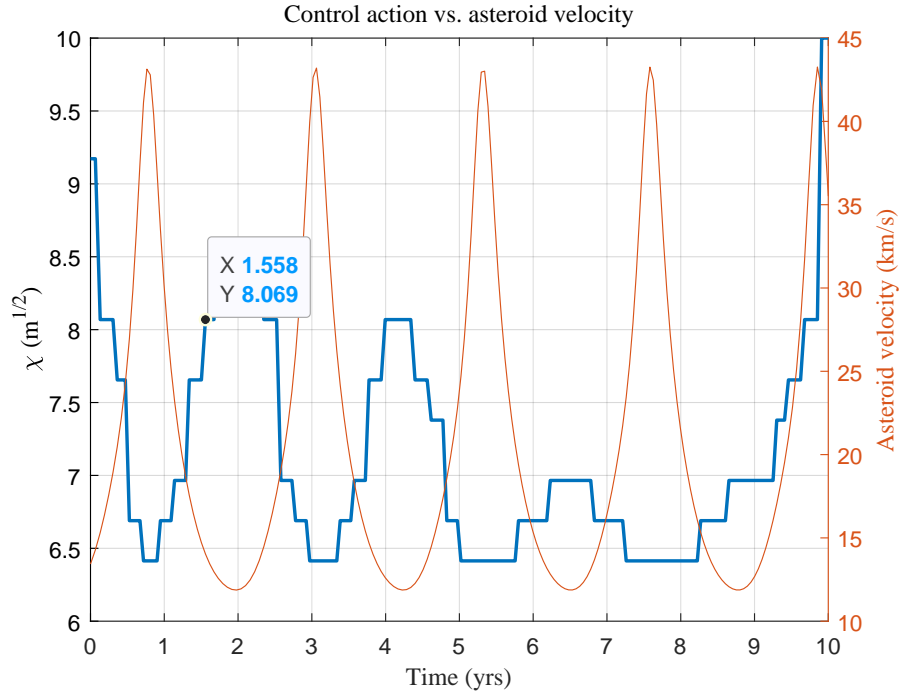


Fig. 7 Time dependence of the control variable r_0, χ for the case of $t_e = 10$ years and its relation to the asteroid velocity.

VII. Conclusions

As a potential method of asteroid impact aversion, the gravity tractor has the advantage of not requiring any direct contact of the spacecraft with the asteroid and therefore avoids problems related to the asteroid’s make-up and structural and material properties. The method relies on the relatively small-magnitude gravitational force that can be exerted on the asteroid by a typically sized spacecraft.

The work presented in this paper describes an approach to increase the efficiency of the gravity tractor by optimizing the amount of mass needed to deflect an asteroid by a given amount. Thus, a decrease of gross spacecraft mass for the same amount of deflection has been obtained that is in the order of 20%. This is a decrease in mass that significantly improves the practicality of the gravity tractor as an approach to asteroid deflection. Thus, for an asteroid of a “smaller size” with a lead time in the order of 5 to 15 years, the gravity tractor on a restricted Keplerian orbit may be a viable option for asteroid deflection.

A limitation of the current study (and other studies regarding the use of gravity tractors) is that it is assumed that the asteroid has a spherically symmetric gravitational field. This is generally not the case, and may require additional asteroid-centric navigation in order to remain in a controlled orbit about the asteroid. This problem is the subject of current studies.

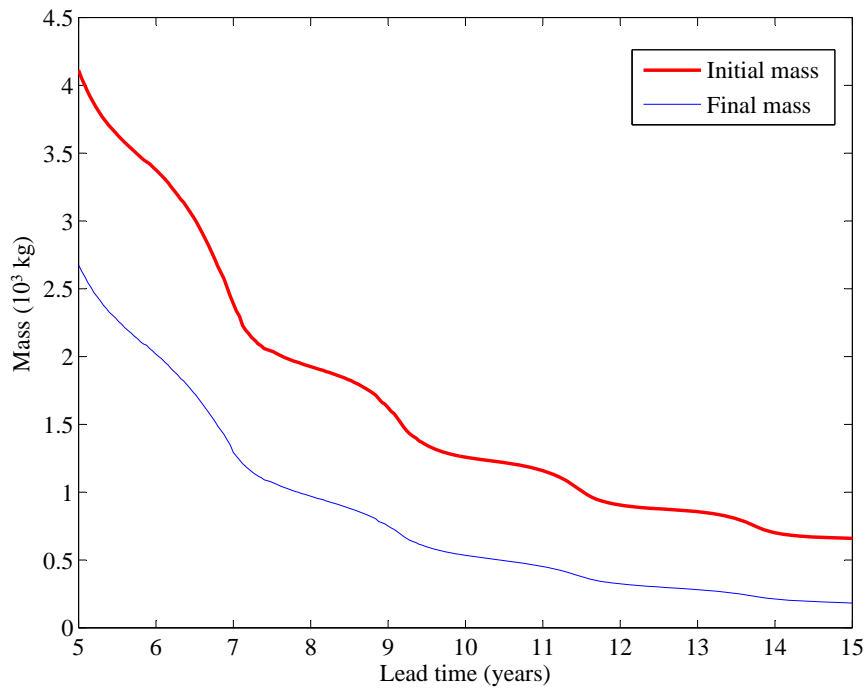


Fig. 8 Optimal wet mass and dry mass for the gravity tractor spacecraft as a function of lead time at start of deflection action.

References

- [1] Ahrens, T., and Harris, A., “Deflection and Fragmentation of Near-Earth Asteroids,” *Nature (London)*, Vol. 360, No. 6403, 1992, pp. 429–433.
- [2] McInnes, C., “Deflection of Near-Earth Asteroids by Kinetic Energy Impacts from Retrograde Orbits,” *Planetary and Space Science*, Vol. 52, No. 7, 2004, pp. 587–590.
- [3] Dachwald, B., and Wie, B., “Solar Sail Trajectory Optimization for Intercepting, Impacting, and Deflecting Near-Earth Asteroids,” *AIAA Guidance, Navigation, and Control Conference and Exhibit, 15-18 August 2005, San Francisco, California*, 2005.
- [4] Dachwald, B., and Wie, B., “Solar Sail Kinetic Energy Impactor Trajectory Optimization for an Asteroid-Deflection Mission,” *Journal of Spacecraft and Rockets*, Vol. 44, No. 4, 2007, pp. 755–764.
- [5] Izzo, D., Bourdoux, A., Walker, R., and Ongaro, F., “Optimal Trajectories for the Impulsive Deflection of NEOs,” *56th International Astronautical Congress, Paper IAC-05-C1.5.06*, 2005.
- [6] Asphaug, E., Ostro, S., Hudson, R., Scheeres, D., and Benzi, W., “Disruption of Kilometre-Sized Asteroids by Energetic Collisions,” *Nature (London)*, Vol. 393, No. 6684, 1998, pp. 437–440.

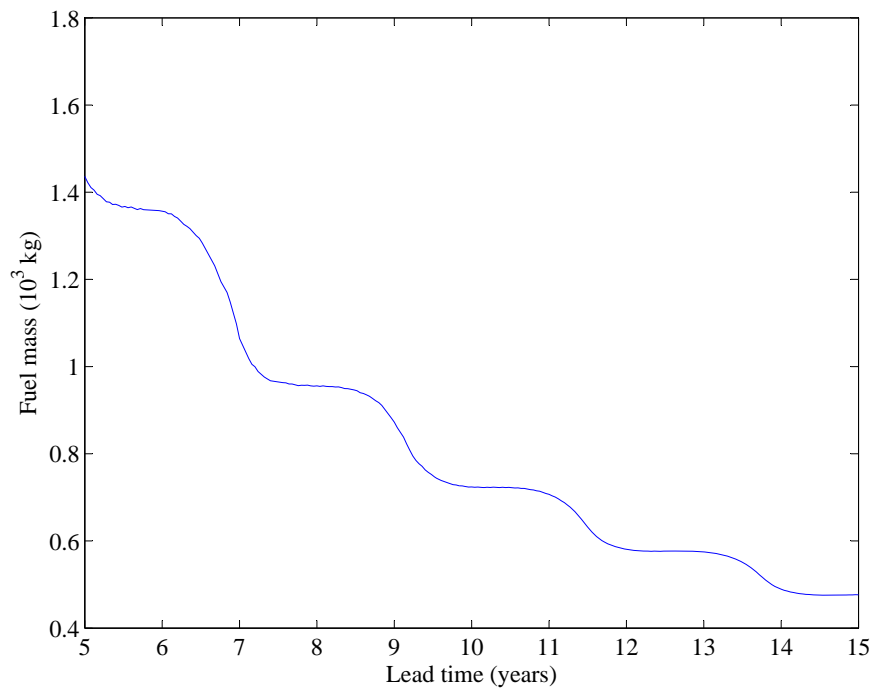


Fig. 9 Optimal fuel mass burned for the gravity tractor spacecraft as a function of lead time of start of deflection action.

- [7] Sanchez, P., Colombo, C., Vasile, M., and Radice, G., “Multicriteria Comparison Among Several Mitigation Strategies for Dangerous Near- Earth Objects,,” *Journal of Guidance, Control, and Dynamics*, Vol. 32, No. 1, 2009, pp. 121–142.
- [8] Dearborn, D., Patenaude, S., and Managan, R., “The Use of Nuclear Explosives To Disrupt or Divert Asteroids,” *Proceedings of the Planetary Defense Conference, Washington, DC, March 5-8, 2007*.
- [9] Lu, E., and Love, S., “Gravitational Tractor for Towing Asteroids,” *Nature*, Vol. 438, No. 7065, 2005, pp. 177–178.
- [10] Gehler, M., Ober-Blobaum, S., Dachwald, B., and Marsden, J., “Optimal Control of Gravity Tractor Spacecraft Near Arbitrarily Shaped Asteroids,” *1st IAA Planetary Defense Conference, Granada, Spain, 27-30 April 2009, 2009*.
- [11] Wie, B., “Dynamics and Control of Gravity Tractor Spacecraft for Asteroid Detection,” *Journal of Guidance, Control, and Dynamics*, Vol. 31, No. 5, 2008, pp. 1413–1423.
- [12] Olympio, J., “Optimal Control of Gravity-Tractor Spacecraft for Asteroid Deflection,” *Journal of Guidance Control and Dynamics*, Vol. 33, 2010, pp. 615–621.
- [13] Fahnestock, E., and Scheeres, D., “Dynamic Characterization and Stabilization of Large Gravity-Tractor Designs,” *Journal of Guidance Control and Dynamics*, Vol. 31, No. 3, 2008, pp. 501–621.
- [14] Foster, C., Bellerose, J., Mauro, D., and Jaroux, B., “Mission concepts and operations for asteroid mitigation involving multiple gravity tractors.” *Acta Astronautica*, Vol. 90, No. 1, 2013, pp. 112–118.
- [15] Ketema, Y., “Asteroid Deflection Using a Spacecraft in Restricted Keplerian Motion,” *Acta Astronautica*, Vol. 136, 2017, pp. 64–79.
- [16] Mazanek, D., Reeves, D., Hopkins, J., Wade, D., Tantardini, M., and Shen, H., “Enhanced gravity tractor technique for planetary defense.” *4th IAA Planetary Defense Conference (PDC 2015) April 2015, Frascati, Roma, Italy, 2015*, pp. 13–17.
- [17] McInnes, C., “Near Earth Object Orbit Modification Using Gravitational Coupling,” *Journal of Guidance, Control, and Dynamics*, Vol. 30, No. 3, 2007, pp. 870–873.
- [18] McInnes, C., “Dynamics, Stability, and Control of Displaced Non-Keplerian Orbits,” *Journal of Guidance, Control, and Dynamics*, Vol. 21, No. 5, 1998, pp. 799–805.
- [19] Gong, S., Li, J., and Yin, H. B., “Formation flying solar-sail gravity tractors in displaced orbit for towing near-Earth asteroids,” *Celestial Mechanics and Dynamical Astronomy*, Vol. 105, No. 1-3, 2009, pp. 159–177.
- [20] Yang, H., Vetrivano, M., Vasile, M., and Zhang, W., “Autonomous navigation of spacecraft formation in the proximity of minor bodies.” *Proceedings of the Institution of Mechanical Engineers, Part G: Journal of Aerospace Engineering*, Vol. 230, No. 1, 2016, pp. 189–204.

- [21] Broschart, S., and Scheers, D., “Control of Hovering Spacecraft Near Small Bodies: Application to Asteroid 25143 Itokawa,” *Journal of Guidance, Control, and Dynamics*, Vol. 28, No. 2, 2005, pp. 345–354.
- [22] Kirk, D. E., *Optimal Control Theory: An Introduction*, Dover Publications Inc., 1998, Chap. 3.
- [23] Lewis, F., and Syrmos, V., *Optimal Control*, John Wiley and Sons, 1995.
- [24] Curtis, H., *Orbital Mechanics for Engineering Students*, 3rd ed., Elsevier Ltd., 2014, Chap. 3.
- [25] Bate, R., Mueller, D., and White, J., *Fundamentals of Astrodynamics*, Dover Publications, 1971.
- [26] Hale, F., *Introduction to Space Flight*, Prentice Hall, 1994.
- [27] Curtis, H., *Orbital Mechanics for Engineering Students*, 3rd ed., Elsevier Ltd., 2014, Chap. 2.
- [28] Hale, F., *Introduction to Space Flight*, Prentice Hall, 1994.
- [29] “NASA Near Earth Object Program: (Retrieved 2021-10-8),” , 2016. URL <https://web.archive.org/web/20131017014439/http://neo.jpl.nasa.gov/risk/2007vk184.html>.
- [30] “JPL Small-Body Database: 2007 VK184: (Retrieved 2021-10-8),” , 2016. URL https://ssd.jpl.nasa.gov/tools/sbdb_lookup.html#/?sstr=2007VK184.